Mass on a spring map for the dripping faucet at low flow rates

L. Renna*
Dipartimento di Fisica dell'Università and Istituto Nazionale di Fisica Nucleare–73100, Lecce, Italy
(Received 24 March 2001; published 24 September 2001)

An improved discrete map for the mass-on-a-spring model for the dripping faucet is used to reproduce the evolution of experimental dripping spectra at low flow rates. If an inverse dependence of drop mass on flow rate is supposed, a repeated evolution from period 1 to chaos is obtained. A comparison between discrete relaxation oscillator attractors and dissipative type-web map attractors is carried out. It is found that a dissipative web map accounts for some characteristics of the relaxation oscillator map, thus giving further tools for investigation.

DOI: 10.1103/PhysRevE.64.046213 PACS number(s): 05.45.−a, 47.20.Ma, 47.52.+j

I. INTRODUCTION

In the last few years, many experiments have demonstrated that the dripping faucet is a classic physical example of complex dynamical behavior. In fact, a large variety of phenomena have been observed, such as period doubling, multiperiodicity, quasiperiodicity, crisis, Hopf bifurcation, inverse cascade, multiple stability, hysteresis, strange attractors, and so forth [1–14].

Attempts at modeling leaky tap dynamics were developed by means of the variable mass-on-a-spring model [1], and more recently through fluid dynamical computations [15,16]. Improved mass-spring models [17–20], achieved by changing the mechanism at the breakup point and the reset conditions, exhibit a variety of complex behavior in good agreement with experiments. The importance of the critical moment [21] is confirmed by the reproduction of dripping dynamics by means of discrete mapping, obtained by approximating the solution of the equation of motion with an analytical function [22,23], and recently with a reversible linear function at the break point [24].

Among other features, dripping faucet experiments have exhibited a structure of period-1 and chaotic states, which repeatedly appears as the flow rate increases. In the range of very small flow rates each structure is composed of period-1 and period-2 motions [6,11,14]. This behavior seems to be a characteristic of leaking from faucets of relatively large diameters for relatively low flow rates.

The alternating structure of stable and chaotic states was roughly obtained from fluid dynamical calculations. The alternating structure of period-1 and period-2 motion in a range of very small flow rates was not reproduced, because long-term simulations take excessive computational time and hence do not yield enough ''data'' [16]. Unfortunately, this is the essential problem involved in fluid dynamical simulations, so that the authors of [16] propose a mass-spring model constructed on the basis of fluid dynamical computation, where the values of the parameters are set only after preliminary execution of fluid dynamical numerical calculations. This adds to the usefulness of the oscillator model. Thus, even if the hydrodynamic approach is a basic tool for the understanding of drop formation and the breakup phenomenon, it needs speeding up in order to predict the lengthy drop sequences observed in experiments.

In this paper it will be demonstrated that improved mass-spring models can reproduce the dynamical behavior at low flux, simply by varying the form of the contributions of physical parameters in different ranges of flow rate. In fact, there is no *a priori* reason for parameters to be constant; they could depend on flow rate or on the physical conformation of the experimental apparatus. If we make the depletion of drop mass depend inversely upon flow rate, we hope to obtain the structure observed experimentally. Preliminary results [25] based on the use of the analytical approximation [22] show indications favorable to this hypothesis.

The spring-mass-based discrete map that was recently proposed to describe the dripping faucet will be used. This simplified model has an analogy with a web-map type [26], where a modification has been made in order to introduce dissipation.

The enormous simplifications in reducing the complex fluid system to a simple oscillator map can help in the understanding of many things, because the model parameters retain their physical meaning, and numerical calculations are straightforward (reducing the computational time) notwithstanding the complexity of the dynamics they produce. Thus investigations performed by means of the improved mass-spring model can cast further light on the dynamical mechanisms that rule the dripping multicomplexity.

The paper develops as follows. In Sec. II the analytical map and in Sec. III the discrete map are reviewed briefly, and their possible improvements are discussed in Sec. IV; simulations at low flow rates are reported in Sec. V. In Sec. VI an analogy with a dissipative web-map type is analyzed; the conclusions are drawn in Sec. VII.

II. THE ANALYTICAL MASS-SPRING MAP

In the relaxation oscillator model a growing mass (a drop), suspended on a spring (surface tension), is subjected to gravitational force and viscous damping [1,17–20]. The displacement of the center of mass (of a drop hanging from an orifice) can be approximately described by the dimensionless equation [22,23]

*Email address: renna@le.infn.it

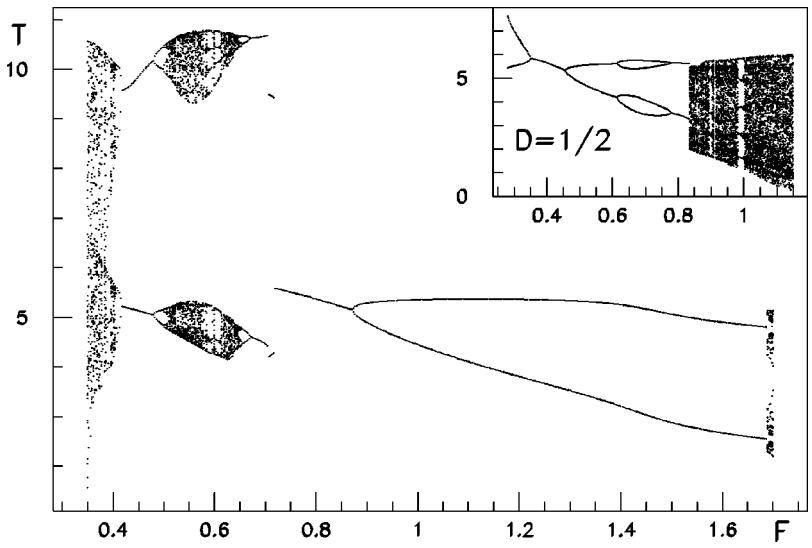

FIG. 1. Bifurcation diagrams obtained from a mass-spring map. The parameter values are $K=10$ and $\alpha=5$. The inset shows a diagram with $D=1/2$. 25×10^4 data points are used (inset 2×10^4 data points).

$$X(T)=\{A\sin[\Omega(T)T]+B\cos[\Omega(T)T]\}e^{-T/M(T)}+M(T)/K, \tag{1}$$

where $\Omega^2(T)=K/M(T)$, the mass is supposed to vary linearly with time $M(T)=m+FT$, K and F are the parameters modeling spring force and flow rate, and the viscosity parameter is normalized to 1.[1]

The breakaway of the drop is simulated by reducing the mass, at the critical point $X_c=1$, by a quantity proportional to its momentum,

$$\Delta M=\alpha M V_c, \tag{2}$$

where α is a parameter, whereas the residual of mass $m=M-\Delta M$ is supposed to restart with velocity V_c at the point

$$X_0=1-R\frac{\Delta M}{M}, \tag{3}$$

where $R=(3\Delta M/4\pi D)^{1/3}$ represents the radius of a spherical drop of density D $(=1)$. Therefore m represents the mass of the residue after the falling of the previous spherical drop. In Ref. [22] a mapping, that is, the series of time intervals between each drop, was obtained by solving numerically the equation $X(T)=1$ (analytical map).

III. THE DISCRETE RELAXATION OSCILLATOR MAP

The analysis of Eq. (1) reveals many qualitative similarities with the effective behavior of drops in a real faucet [9]. In Ref. [24], where investigations about such analogies showed the relevance of the dynamics at the break-off point, a discrete map was proposed that reproduces the behavior observed in real systems. The map is much simpler then the analytical map obtainable by means of Eq. (1), which requires the numerical solution of a nonlinear equation. The map can be written as follows:

$$m_{n+1}=(m_n+FT_n)(1-\alpha V_n), \tag{4}$$

$$x_{n+1}=1-\left[\frac{3\alpha}{4\pi}(m_n+FT_n)V_n\right]^{1/3},$$

$$v_{n+1}=V_n,$$

where

$$V_n=V(m_n,v_n,x_n,T_n) \tag{5}$$

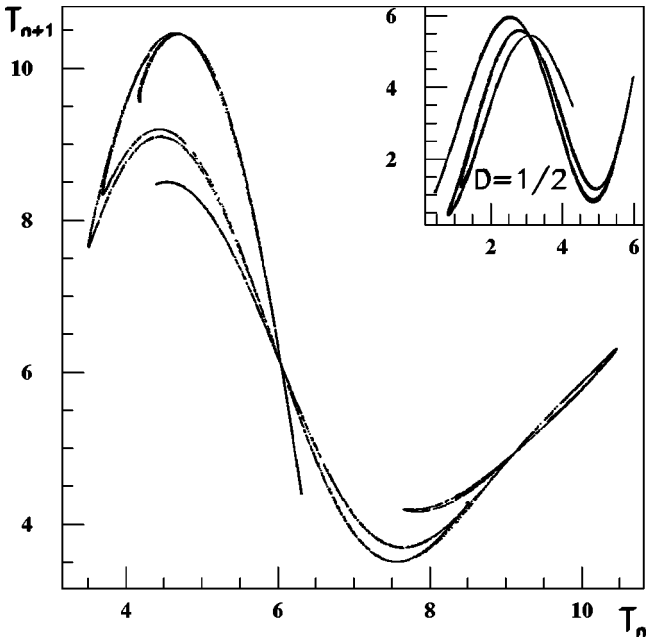

FIG. 2. Plots of return maps at $F=0.37$, $D=1$ and $F=1.1$, $D=1/2$ (inset). K and α values are as in the previous figure. 10^4 data points are used.

[1]Equation (1) is a simplified form, because the term VdM/dt in mass-spring equations of motion is neglected. In the complete form, the term $-T(1+F)/M$ appears as the argument of the exponential. This term permits calculations to be performed for a wider range of the flow rate.

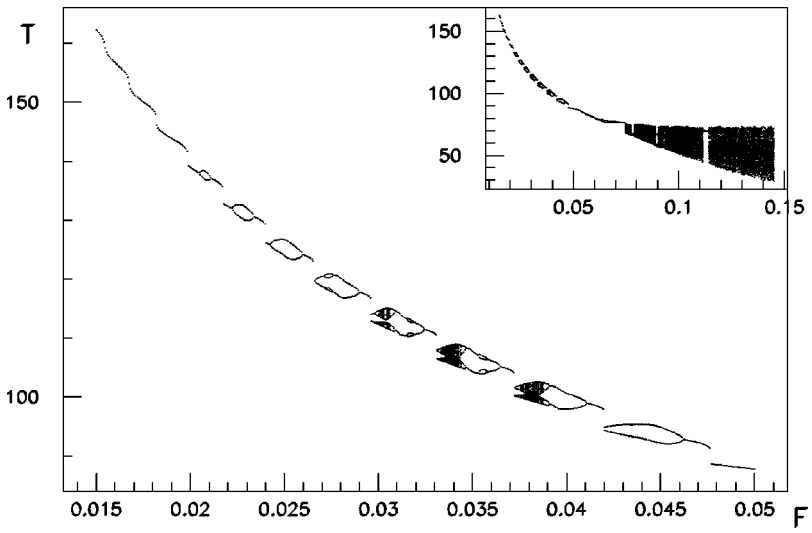

FIG. 3. Enlargement of a bifurcation diagram (shown in the inset) in a range of low flow rate. Parameter values are $K=18,\ \alpha_0=20,\ \gamma=1/2$.

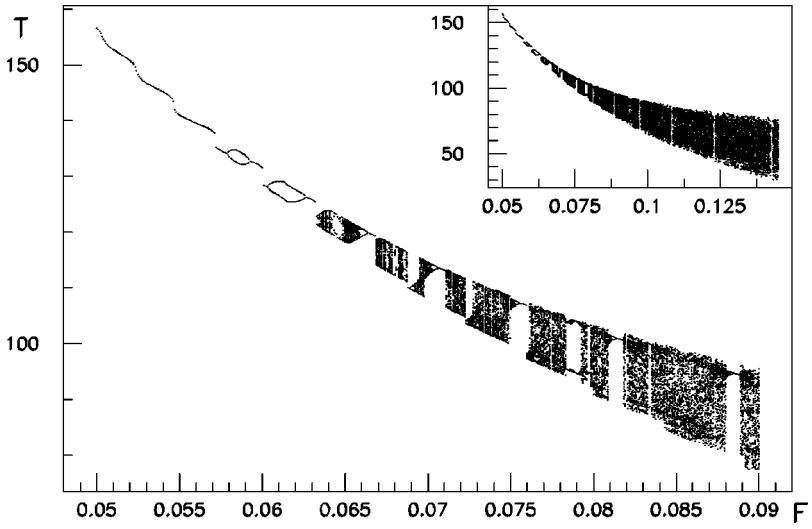

FIG. 4. Same as in Fig. 3 but for different values of parameters: $K=18,\ \alpha_0=8,\ \gamma=1$.

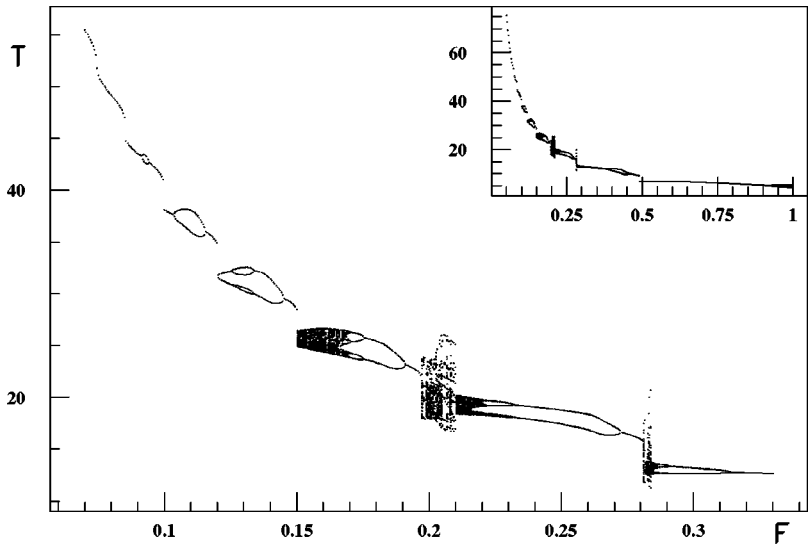

FIG. 5. Same as in Fig. 4 but for different values of parameters: $K=10,\ \alpha_0=5,\ \gamma=0.92$.

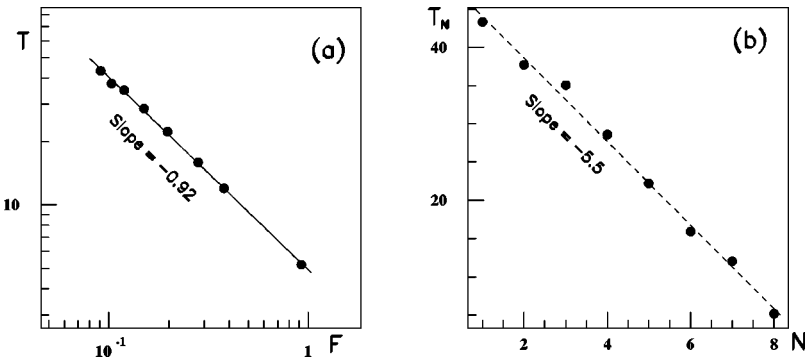

FIG. 6. (a) The log-log plot of transition time intervals T versus F. (b) The plot of transitional T as a function of the transition point number N. The straight line fits are shown.

is the velocity of the falling drop at the break-off moment,

$$T_n = \frac{K - m_n}{F + v_n} \tag{6}$$

is the nth drop time interval, which is the quantity measured in experiments, and m_{n+1}, and x_{n+1}, v_{n+1} are the initial mass, position, and speed of the $(n+1)$th drop, respectively. The velocity is given by

$$V(T) = [(Ac - Bd)\cos\Omega T - (Bc + Ad)\sin\Omega T]e^{-T/M(T)} + F/K, \tag{7}$$

where $c(T) = \Omega(1 - FT/2M)$ and $d(T) = (1 - FT/M)/M$. Details are reported in [24].

IV. POSSIBLE IMPROVEMENTS

There are several ways to implement the oscillator map. In Ref. [20] the effects of changing the breakup mechanism were analyzed. In Ref. [24] it was observed that the model parameters K and α could depend on the dynamical state of the faucet, and in Ref. [23] a variation of the density parameter D was suggested, since it controls the rebound. We call *external* any change that introduces some dependence of these parameters on the flow rate (that is, the physical control parameter in the experiments), whereas different changes that make parameters depend on dynamical quantities, such as mass or velocity, will be called *internal*.

A typical bifurcation diagram obtained with map (4) at given values of the parameters (K, α) is shown in Fig. 1. The inset shows the plot corresponding to the spectrum with $D = 1/2$. Notice that the system undergoes a wide variety of transitions. The parameter D depends on the liquid density, but the effect of lowering D, in the mass-spring model, is to enhance the rebound, so that the bifurcation diagrams show a different variety of structures in the ranges of allowed flow rates. This is an example of how an external change can be realized. Dripping spectra are calculated by increasing F, and the final state, at a given F value, is chosen as the initial state at the next value in order to override instabilities due to coexistence of attractors (the standard initializing values we used are $x_0 = 0.01$, $v_0 = 0.001$).

In Fig. 2 the plots of typical return maps, obtained from the previous spectra, are reported. Notice the evident layered structure of the attractors.

V. SIMULATIONS AT LOW FLOW RATES

A repeating period-1 structure of the bifurcation diagram has been found experimentally with nozzles of large diameter ($\gtrsim 5$ mm), for slow flow rates [6,11,14]. In these circumstances, the volume of impelling fluid pushes the drop down weakly and the forming drop mass grows slowly. The restoring force and viscosity oppose the effect of gravity, so that it takes a long time before the drop separates by its own weight. This causes any information about the previous drop to be lost, resulting in a monotonic dependence of the drip time interval and flow rate. In fact, in experiments it is found that large drops leave the nozzle at a constant rate, resulting in a period-1 attractor, or a large drop followed by a tiny one is produced. As the flow rate is increased, the drop size varies slightly and the time between drops varies in a nonlinear manner [5]. The resulting dripping spectrum shows period-2 structures included between period-1 behaviors. The whole evolves toward a chaotic pattern.

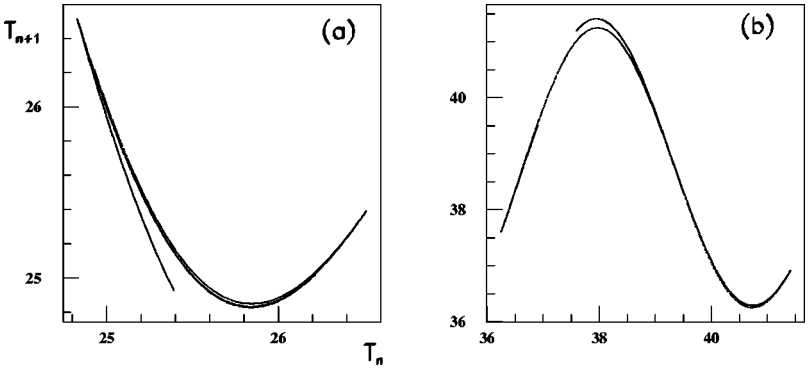

FIG. 7. Two return maps at low flow rates. The sets of parameters are (a) $K = 10$, $\alpha_0 = 5$, $\gamma = 0.92$, $F = 0.152$, (b) $K = 10$, $\alpha_0 = 7$, $\gamma = 1.111$, $F = 0.2$.

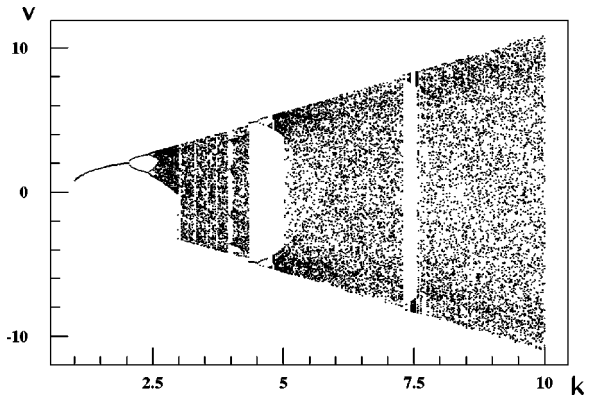

FIG. 8. Plot of the bifurcation diagram of the dissipative web map versus the control parameter k. The dissipative parameter is set to $h=0.1$.

In the attempt to describe the growing drop with Eq. (1) by means of numerical calculations, we found that, when the flow rate is very small, the drop oscillates weakly near $X=1$ (as is expected) with a slow velocity, so that the depleted mass as given by Eq. (2) is also small. This effect is relevant as flow rates become very low, and it affects the quantity of depleted mass. Thus a simple description with Eqs. (4)–(6) is inadequate: successive numerical iterations cannot continue, as m_n immediately becomes greater than K [see Eq. (6)].

On the other hand, as remarked in the previous section, it is reasonable that the depleted mass can depend somehow on F. Thus, in order that the falling drop mass be raised at low flow rates, we introduce in Eq. (2) and in Eqs. (4) a dependence of α on some inverse power of F, such as

$$\alpha(F)=\alpha_0/F^{\gamma}. \tag{8}$$

In the insets of Figs. 3 and 4 plots of dripping spectra, obtained with $\gamma=1/2$ and 1, respectively, show the experimentally observed sequence: areas with stable dripping behavior alternate with areas of chaotic behavior. Details are visible in the larger parts of the figures, where period-1 structures repeatedly appear when the flow rate is varied.

Katsuyama and Nagata [14] have observed that the experimental drip intervals decrease as $T_n \propto F_n^{-0.92}$, where F_n are the flow rates at the transition points at which the period-1 state undergoes a transformation with increasing F. Moreover, they found experimentally that the volume (mass) of the drip increases with F.

A linear fit on a log-log scale of time intervals of the bifurcation diagram of Fig. 3 gives a mean slope of about 0.5 and a slope of -0.45 for the 12 transition points. The bifurcation diagram of Fig. 4 has 13 transition points. On a log-log scale a linear fit gives a straight line with slope equal to -0.73. If the first six points are utilized, the slope is equal to -0.92, in agreement with the experimental data. Thus, for $F \gtrsim 0.075$ the simulation does not comply entirely with real dripping behavior at the low flow rates of Ref. [14]. We have made several computer simulations at different values of the parameters (K,α_0). A detailed analysis shows the following facts: with increasing flow velocity, the time intervals decrease on average as $F^{-\gamma}$ and an almost similar decrease is found for the transitional time intervals, even though these show some dependence on the (K,α_0) values. Thus the hypothesis of an inverse dependence of α on F, with an exponent $\gamma \approx 1$, is correct, as many experimental facts are qualitatively reproduced. Moreover, we are able also to get quantitative agreement with experimental results. In Fig. 5 (inset) a bifurcation diagram, evaluated with the same (K,α_0) values as those of Fig. 1 and with $\gamma=0.92$, is reported. In the enlarged plot we can observe a dynamical evolution very similar to the experimental ones with period-1 behavior that alternates with period-2 or chaotic behavior.

Each period-1 structure occurs periodically, showing a scaling law that has been found experimentally [6,14]. Figure 6(a) reports the log-log plot of transition points versus F and Fig. 6(b) shows the plot of transition points against N, where N is a transition point number. The linear fit indicated in (a) gives

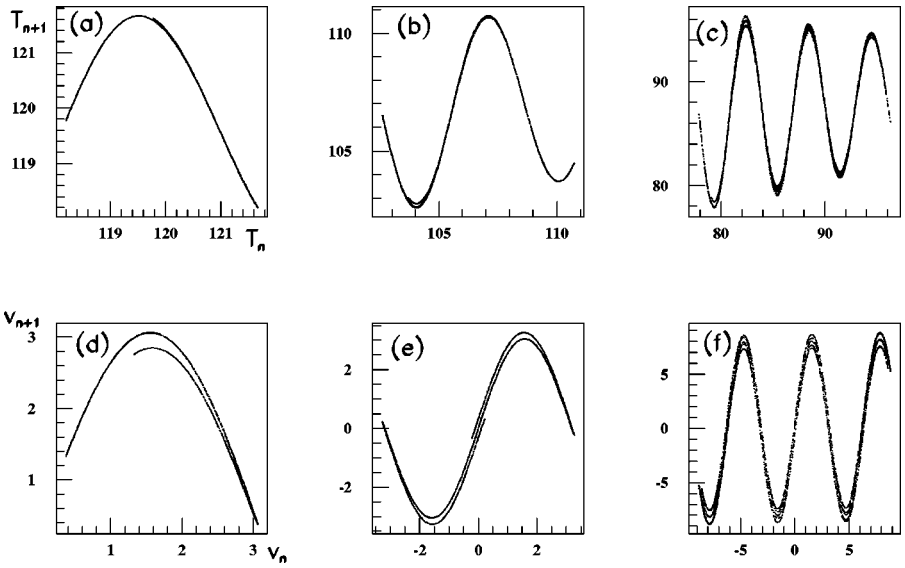

FIG. 9. Comparison between mass-spring maps (first three plots, with $K=18$, $\alpha_0=8$, $\gamma=1$) and web maps (last three, with $h=0.1$) for different values of control parameters. $F=$(a)0.0654, (b) 0.073, (c) 0.089; $k=(d)2.8$, (e) 3.0 (f) 8.0.

$$T \propto F^{-0.92} \tag{9}$$

whence the volume of the drip increases with F as $FV \propto F^{0.08}$. The fit in Fig. 6(b) can be expressed as

$$T_N = 49.5 - 5.5F. \tag{10}$$

The scaling law (9) agrees exactly with the experimental scaling law obtained in Ref. [14]. Equation (10) corresponds to the periodicity of the period-1 structures. Analogous simulations with the scaling law (9) can be obtained with different sets of parameters, for example, $K=10$, $\alpha_0=7$, and $\gamma=1.111$.

Finally, plots at low F of two return maps show chaotic attractors of low dimension in accordance with the experimental ones (Fig. 7). Return maps obtained for higher flow rates will be discussed in the subsequent section.

The present model fails to reproduce all the experimental features. In effect, in the period-1 region the experimental time interval T_n increases with F. Perhaps the reason is that vibrations can affect the behavior of T_n in a complicated way that can also depend on the flow rate. We think the actual behavior can be achieved by performing *internal* improvements. This is suggested also from the mass-spring model constructed on the basis of fluid dynamical computations, where a dependence of K on the mass of the forming drop is supposed [16]. Studies are in progress in order to test this hypothesis.

VI. A DISSIPATIVE WEB MAP

The return maps show a reduction of dimensionality at low flow rates. On increasing F, the complexity of their structure rises, and this behavior is in agreement with experiments. However, when the condition (8) is used, often the form of attractors evolves toward a pronounced oscillatory structure, as F is increased. This seems to be the effect of a dominance of the oscillatory term of velocity (7) in the mapping equations (4). This observation suggests an analogy with a web map [26], where an adjustable dissipative factor h is introduced:

$$u_{n+1} = v_n, \tag{11}$$

$$v_{n+1} = hu_n + k\sin(v_n).$$

The web map corresponds to a periodically kicked charged particle rotating in a magnetic field. Figure 8 shows a bifurcation diagram of v_n against k obtained from the map (11) with $h=0.1$. On increasing the control parameter k the system follows a period doubling route to chaos. The spectrum produces a variety of transitions and attractors of increasing complexity. The analogy with the dripping faucet map (4) is explained in Fig. 9 where three attractors obtained at different values of flow rate are compared with attractors calculated at different value of the control parameter k. Notice the agreement between the forms of corresponding attractors. This accord is not casual, because of the strict analogy between the mass-on-a-spring model and classical kicked rotors. As k falls, the effect of the oscillatory term in Eq. (8) is reduced. This corresponds to low flow rate dripping, where the gravity force competes with surface tension, so that slow oscillations characterize the fluid pendent from the faucet. At higher flow rates, the recoil of the stretched liquid leading to break-off is enhanced, as the oscillations in the residue are not damped completely before the next drop detaches. These oscillations are realized in the web map at high k. The return maps at low flow rate [plots 9(a) and 9(b)] have a behavior that is characteristic of the real leaky tap.

VII. CONCLUSIONS

We introduced an improved mass-spring map that succeeded also in reproducing qualitatively the dynamical behavior of dripping faucets observed in experiments at low flow rate. The agreement of the model with experimental data can be made quantitative. An analogy of behavior suggested a possible connection between the dynamics of the spring-mass map and a modified web map that is related to a rotor subjected to a periodically pulsed field. We showed that the mass-on-a-spring model remains so far an unequaled tool for the simulation and study of dripping faucet dynamics owing to its very short computational time and its flexibility in allowing improvements, although the analysis of the system from the point of view of fluid mechanics is always desirable.

ACKNOWLEDGMENT

This work was supported in part by COFIN 2000 ''Sintesi.''

[1] P. Martien, S.C. Pope, P.L. Scott, and R.S. Shaw, Phys. Rev. Lett. **110A**, 399 (1985).
[2] H.N. Núñez Yépez, A.L. Salas Brito, C.A. Vargas, and L.A. Vicente, Eur. J. Phys. **10**, 99 (1989).
[3] X. Wu and Z.A. Schelly, Physica D **40**, 433 (1989).
[4] R.F. Cahalan, H. Leidecker, and G.D. Cahalan, Comput. Phys. **4**, 368 (1990).
[5] K. Dreyer and F.R. Hickey, Am. J. Phys. **59**, 619 (1991).
[6] J. Austin, Phys. Lett. A **155**, 148 (1991).
[7] J.C. Sartorelli, W.M. Gonçalves and R.D. Pinto, Phys. Rev. E **49**, 3963 (1994).
[8] R.D. Pinto, W.M. Gonçalves, J.C. Sartorelli, and M.J. de Oliveira, Phys. Rev. E **52**, 6896 (1995).
[9] M.S.F. da Rocha, J.C. Sartorelli, W.M. Gonçalves, and R.D. Pinto, Phys. Rev. E **54**, 2378 (1996).
[10] J.G. Marques da Silva, J.C. Sartorelli, W.M. Gonçalves, and R.D. Pinto, Phys. Lett. A **226**, 269 (1997).
[11] T. Schmidt and M. Marhl, Eur. J. Phys. **18**, 377 (1997).
[12] W.M. Goncalves, R.D. Pinto, J.C. Sartorelli, and M.J. de Oliveira, Physica A **257**, 385 (1998).
[13] R.D. Pinto, W.M. Gonçalves, J.C. Sartorelli, I.L. Caldas and M.S. Baptista, Phys. Rev. E **58**, 4009 (1998).
[14] T. Katsuyama and K. Nagata, J. Phys. Soc. Jpn. **68**, 396 (1999).

[15] N. Fuchikami, S. Ishioka, and K. Kiyono, J. Phys. Soc. Jpn. **68**, 1185 (1999).
[16] K. Kiyono and N. Fuchikami, J. Phys. Soc. Jpn. **68**, 3259 (1999).
[17] G.I. Sánchez Ortiz and A.L. Salas Brito, Phys. Lett. A **203**, 300 (1995).
[18] G.I. Sánchez Ortiz and A.L. Salas Brito, Physica D **892**, 151 (1995).
[19] A. D'Innocenzo and L. Renna, Int. J. Theor. Phys. **35**, 941 (1996).
[20] A. D'Innocenzo and L. Renna, Phys. Rev. E **55**, 6776 (1997).
[21] P.A. Bernhardt, Physica D **52**, 489 (1991).
[22] A. D'Innocenzo and L. Renna, Phys. Lett. A **220**, 75 (1996).
[23] A. D'Innocenzo and L. Renna, Phys. Rev. E **58**, 6847 (1998).
[24] L. Renna, Phys. Lett. A **261**, 162 (1999).
[25] L. Renna, *Proceedings of the Workshop Nonlinearity, Integrability and All That, Twenty Years After NEEDS '79*, edited by M. Boiti, L. Martina, F. Pempinelli, B. Prinari, and G. Soliani (World Scientific, Singapore, 2000), p. 511.
[26] G.M. Zaslavsky and B.A. Niyazov, Phys. Rep. **283**, 73 (1997).